c-axis conduction in graphite intercalation compounds

Ko Sugihara
Center for Materials Science and Engineering, Massachusetts Institute of Technology, Cambridge, Massachusetts 02139
(Received 7 August 1987)

In an earlier paper, we introduced the concepts of phonon-assisted and impurity-assisted hopping processes to explain the c-axis resistivity in graphite intercalation compounds (GIC's). A different theory was proposed by Shimamura. Both theories provide a qualitative explanation for the observed behaviors in low-stage compounds but they cannot account for the high-temperature behavior in high-stage compounds. In this paper two new mechanisms are introduced. One is the interaction of the carriers with the LO phonons polarized along the c axis. This is important in low-stage compounds with large charge transfer. The other mechanism is the scattering of the carriers by stacking faults, which is important in high-stage compounds. By considering the mechanisms proposed previously by us and by Shimamura together with the new mechanism, we obtain a qualitative explanation for the temperature and stage dependences of the c-axis resistivity in GIC's.

I. INTRODUCTION

Measurement of the c-axis conductivity σ_c at room temperature in graphite intercalation compounds (GIC's) yields very small values of σ_c ranging from $\sim 10^{-1}$ to 10 $(\Omega\,\mathrm{cm})^{-1}$.[1-9] If we apply the simple Drude formula $\sigma_c = ne^2 l/\hbar k_c$, it yields a mean free path $l_c \ll 10^{-8}$ cm. This implies that σ_c is too small to apply the standard Boltzmann-Bloch formalism.

Most of the c-axis resistivity behavior in low-stage compounds is metallic, while in high-stage compounds the resistivity ρ_c decreases with increasing temperature (see Figs. 1 and 2). Though this behavior is a common feature in GIC's, some kinds of low-stage compounds exhibit a maximum around 150–200 K in the ρ_c versus T curve[4-8] and this behavior is shown in Figs. 3 and 4.

Two theories have been presented to explain the temperature dependence of σ_c in GIC's. One is due to us,[10] and the other is Shimamura's theory.[11] Our theory proposed two mechanisms: (i) an impurity-assisted hopping process and (ii) a phonon-assisted hopping process. The transition across the intercalated layers is described by a transfer Hamiltonian. In low-stage compounds mechanism (i) makes the dominant contribution to ρ_c and it explains qualitatively the observed temperature dependence of ρ_c. Though the temperature dependence expected from mechanism (ii) is similar to the one in high-stage compounds, its magnitude is too small to account for the observed values.

Shimamura proposed a different theory from ours,[11] which involves two mechanisms: (1) the transition across the intercalant layers which is attributed to conduction paths (conduction channels) associated with the structural imperfections, and (2) the interlayer transition process which accompanies phonon emission and absorption. The first process makes an important contribution to ρ_c in low-stage compounds, while mechanism (2) provides values of σ_c too small to explain the observed data in high-stage compounds. Accordingly, neither theory satisfactorily accounts for the observed behavior in the temperature dependence of the c-axis conduction.

In this paper we introduce two new mechanisms: (A) the interaction of the carriers with the LO phonons polarized along the c axis and (B) the scattering of the carriers by stacking faults. Mechanism (A) plays a role in

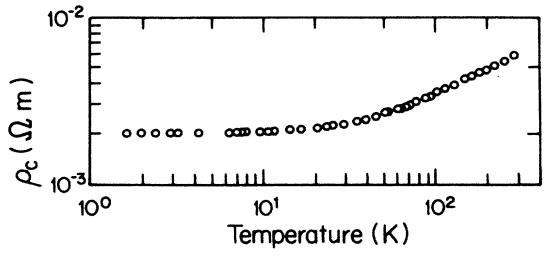

FIG. 1. Temperature variation of the c-axis resistivity of a stage-2 $FeCl_3$ GIC (Ref. 1).

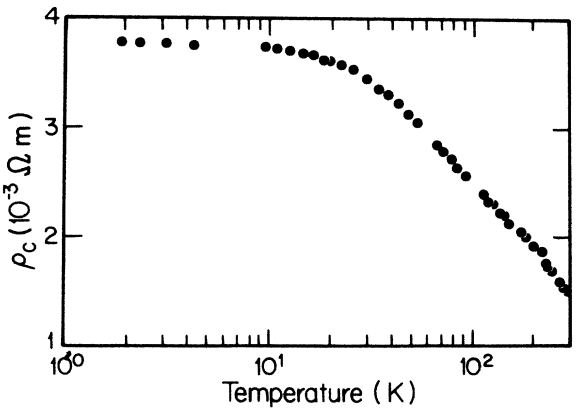

FIG. 2. Temperature dependence of the c-axis resistivity of stage-5 potassium GIC (Ref. 1).

 ©1988 The American Physical Society

low-stage compounds with large charge transfer. Ono pointed out that the electron-wave reflection by the stacking faults associated with the basal dislocation ribbons enhances the c-axis resistivity in graphite.[12] This mechanism explains the resistivity anisotropy ρ_c/ρ_a ranging from $\sim 10^2$ to $\sim 10^5$. The theory predicts that ρ_c exhibits a metallic temperature dependence, while the observed resistivity shows a maximum around 50 K and decreases with increasing temperature above ~ 50 K.[13,14] This inconsistency can be removed by introducing a thermally activated process over an effective potential barrier associated with the stacking faults. This mechanism is favorable for explaining the resistivity decrease at high temperature in graphite. Since the graphite interior layers of high-stage GIC's are similar to pristine graphite, the same mechanism is expected to be operative in GIC's.

In this paper we show that the temperature and stage dependences of the c-axis resistivity in low-stage and high-stage compounds, except the compounds exhibiting a maximum in ρ_c versus T curves, are well explained in terms of the impurity-assisted hopping process, the conduction-path mechanism, interaction of the carriers with the LO phonons, and scattering by stacking faults.

In Sec. II the phonon-assisted hopping process is discussed and we refer to the impurity-assisted hopping process and the scattering by stacking faults in Sec. III. In the same section the conduction-path mechanism is reformulated. Comparison with the experimental results is made in Sec. IV. Finally, the conclusions are summarized in Sec. V.

II. PHONON-ASSISTED HOPPING PROCESS

The current density or the conductivity is given by

$$\mathbf{j}_c=\sigma_c\mathbf{E}=\frac{e}{\Omega}\sum_{\mathbf{k}} v_d(\mathbf{k}) , \tag{2.1}$$

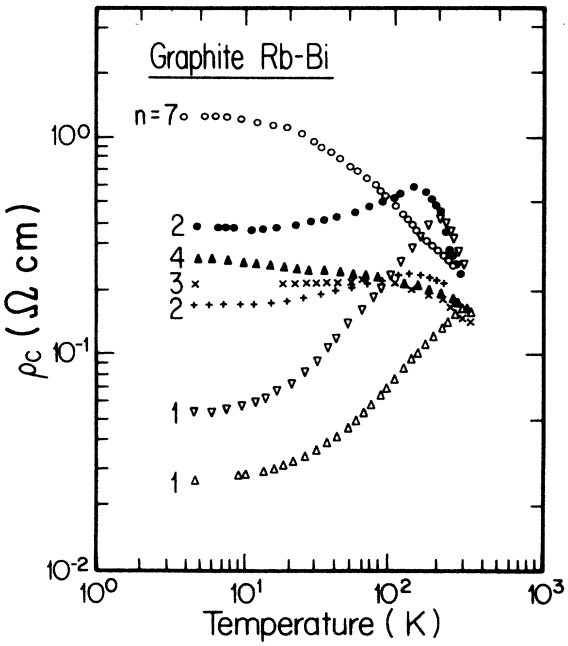

FIG. 3. Temperature dependence of the c-axis resistivity of Rb-Bi GIC's of stages 1–7 (Refs. 4–7).

where $\mathbf{E}$ is an applied field along the c axis and Ω is the sample volume. The drift velocity $v_d(\mathbf{k})$ takes the form[10]

$$v_d(\mathbf{k})=z_0\sum_p [W(n,k\rightarrow n+1,p)-W(n+1,p\rightarrow n,k)] , \tag{2.2}$$

where W represents a hopping rate across the intercalant layer and z_0 is an average hopping distance along the c axis. An explicit form for W is given in the Appendix.

The c-axis conductivity derived from Eqs. (2.1) and (2.2) is composed of three contributions:

$$\sigma_c=(\sigma_c)_{\mathrm{LO}}+(\sigma_c)_{\mathrm{LA}}+(\sigma_c)_I , \tag{2.3}$$

where LO, LA, and I denote the longitudinal-optical phonon, the longitudinal-acoustic phonon, and the ionized impurity, respectively. Expressions for the interactions for the three contributions are given in the Appendix. Equation (2.3) describes the conduction process related to the bounding layers between which an intercalant layer is sandwiched. To obtain the total resistivity, it is necessary to include the contribution from the interior layers. Since more than 90% of the charge transferred from the intercalant to the graphite layers is located on the graphite bounding layers due to the strong Coulomb screening,[15–17] the total resistivity can be approximated by the following formula:[11]

$$\rho_c\simeq\frac{1}{n}[\rho_c(\mathrm{GIG})+(n-1)\rho_c(\mathrm{GG})] , \tag{2.4}$$

where n is the stage number. $\rho_c(\mathrm{GIG})$ stands for the resistivity given by the inverse of Eq. (2.3) and $\rho_c(\mathrm{GG})$ denotes the resistivity associated with the transition between adjacent graphite layers. In low-stage compounds $\rho_c(\mathrm{GIG})$ makes a dominant contribution to ρ_c, while in high-stage compounds $\rho_c(\mathrm{GG})$ term is important.

At first, we consider $(\sigma_c)_{\mathrm{LO}}$ in Eq. (2.3). In general the (0,0,1) phonons polarized along the c axis consist of one acoustic branch and n optical branches in GIC's, where n is the stage number.[18–22] One of the optical branches is a polarization wave where the graphite layers and intercalant layers displace in antiphase, and the associated dipole field scatters the carriers. Since the carriers in GIC's

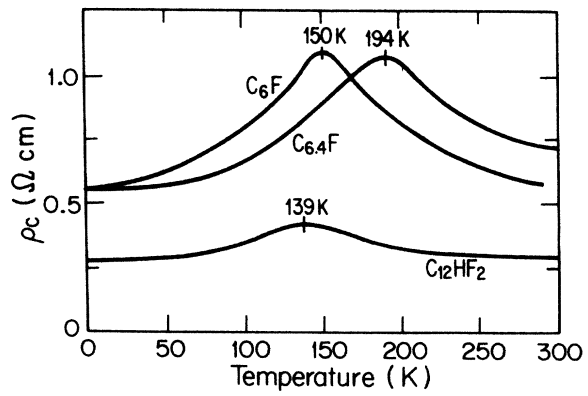

FIG. 4. Temperature dependence of the c-axis resistivity of low-stage fluorine compounds (Ref. 8). Measurement for C_6F is due to Selig *et al.*

are 2D-like, the screening effect on the dipole field is negligible. The interaction between the carriers and the LO phonons with wave vector q is given in the Appendix. The calculation of $(\sigma_c)_{\rm LO}$ is performed along a similar procedure to that used previously.[10] After a lengthy calculation, we obtain

$$(\sigma_c)_{\rm LO}\simeq\frac{32\pi^2\hbar e^2}{k_BT}\frac{(Jee^*)^2}{M^*}\times\frac{E_F^3}{\bar{q}_a p_0^6}\left[\frac{1}{\Gamma}\right]\frac{1}{\exp(\Theta/T)-1}\ , \tag{2.5}$$

where J denotes the transfer integral across the intercalant layers associated with the transfer Hamiltonian, M^* the reduced mass related to the LO vibration, and e^* stands for the effective charge which is proportional to the charge-transfer factor f per intercalant (see the Appendix). E_F is the Fermi energy and Γ is the collision broadening which is included in the energy denominator of the transition rate W in Eq. (2.2) (see the Appendix). p_0, $\bar{q}_a$, and Θ are given as follows: $p_0=(3^{1/2}/2)\gamma_0 a(\gamma_0=3.16$ eV), $\bar{q}_a$ is the average of the LO-phonon wave vector

$$q_a=(q_x^2+q_y^2)^{1/2}\ ,$$
$$\text{and} \tag{2.6}$$
$$k_B\Theta=\hbar\omega_{\rm LO}\ .$$

It should be noted that $\hbar/\Gamma=\tau_{\rm coll}$ is not identical to the relaxation time τ associated with the in-plane resistivity ρ_a, since $1/\tau_{\rm coll}$ does not include a factor limiting the forward scattering. However, for simplicity Γ is estimated from the observed in-plane resistivity in the following. The phonon factor $[\exp(\Theta/T)-1]^{-1}$ makes $(\sigma_c)_{\rm LO}$ small at low temperature ($T\ll\Theta$) but at high temperature $T/\Theta\gtrsim 1$ $(\sigma_c)_{\rm LO}$ becomes important. Equation (2.5) is compared with the observed resistivity for the stage-1 Rb-Bi GIC's in Fig. 3. The following set of parameters is inserted into Eq. (2.5) (J from Ref. 10):

$$J=0.005\text{ eV},\quad E_F=0.8\text{ eV}\ ,$$
$$\bar{q}_a=10^7\text{ cm}^{-1},\quad \Gamma=1.2\times10^{-15}\text{ ergs}\ , \tag{2.7}$$

to obtain

$$\rho_c=0.024(m/2f)^2[\exp(\Theta/T)-1]\ \Omega\,\text{cm}\quad(m=4)\ , \tag{2.8}$$

where the chemical formula for the GIC is assumed to be C_mI (I: intercalant). If $\Theta=T=100$ K and $f=1$ are employed, Eq. (2.8) yields

$$\rho_c=0.17\ \Omega\,\text{cm}\ , \tag{2.9}$$

which is in qualitative agreement with the observed result. In Eq. (2.7) Γ is estimated from the observed resistivity $\rho_a(100\text{ K})=1.25\ \mu\Omega\,\text{cm}$ (see Fig. 5) by using the formula $\rho_a=m^*/ne^2\tau$, where $\Gamma=\hbar/\tau$, $m^*=\hbar k_F/v_F$, $n=k_F^2/\pi I_c$, and $E_F=p_0k_F$. LO frequencies for various GIC's are in the range $\Theta=\hbar\omega_{\rm LO}/k_B\simeq 100$–$150$ K.[18–22]

Next, $(\sigma_c)_{\rm LA}$ is estimated. The coupling constant D for the electron-phonon interaction associated with the out-of-plane vibration was evaluated to be ~4 eV in graphite.[23] It has been recently ascertained that the in-plane resistivity in low-stage compounds below 150 K is well explained in terms of the interaction with the out-of-plane vibration.[24,25] Discrepancies above 150 K are removed by introducing the interpocket scattering process suggested by Kamimura *et al.*[26]

The contribution from the bounding layers to $(\sigma_c)_{\rm LA}$ was obtained in the previous paper:[10]

$$(\sigma_c)_{\rm LA}\simeq\frac{2e^2}{\pi^2}\left[\frac{z_0}{I_c}\right]^2\left[\frac{\Omega}{N}\right]\frac{(DJ)^2}{p_0^6}\frac{q(T)^2F(\Theta/T)E_F^3}{dv_s\Gamma}\ , \tag{2.10}$$

where

$$q(T)=\frac{k_BT}{\hbar v_s},\quad F(\Theta/T)=\int_0^{\Theta/T}dx\,x(e^x-1)^{-1}\ ,$$
$$k_B\Theta=\hbar v_s q_{\max}\ . \tag{2.11}$$

The sound velocity v_s in GIC's depends on both the intercalant species and stage number[18–22] and its magnitude ranges from $\sim2\times10^5$ to $\sim4\times10^5$ cm/sec. I_c represents the c-axis repeat distance and N is the number of unit cells, where the unit cell is defined as the volume including two carbon atoms sandwiched by intercalant layers. Equation (2.10) seems to be ineffective for high-stage compounds, since it is proportional to I_c^{-2}. However, after checking the procedure used in the previous calculation,[10] we obtain an expression of $(\sigma_c)_{\rm LA}$ which does not include I_c. Since σ_c given by Eq. (2.3) comes from the bounding layer, the sample volume Ω in Eq. (2.1) should be replaced by $\Omega(d_0/I_c)$, where d_0 is the distance

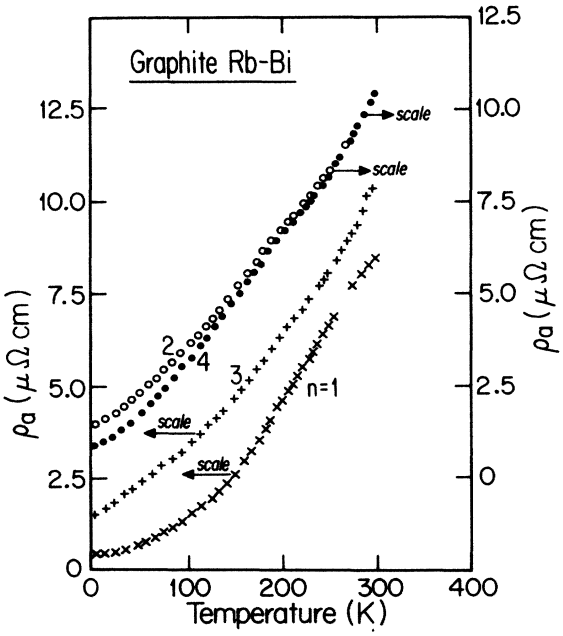

FIG. 5. Temperature dependence of the in-plane resistivity for Rb-Bi GIC's of stages 1–4 (Ref. 4).

separating two graphite layers between which an intercalant layer is sandwiched. Accordingly, we have

$$\left[\frac{z_0}{I_c}\right]^2\frac{\Omega}{N}\rightarrow\left[\frac{z_0}{I_c}\right]^2\frac{I_c}{d_0}\frac{\Omega}{N}=\left[\frac{z_0}{d_0}\right]^2 v_c\ , \tag{2.12}$$

where v_c is the unit-cell volume which is defined as the volume including two carbon atoms sandwiched by intercalant layers. Therefore, Eq. (2.10) becomes

$$(\sigma_c)_{\rm LA}\simeq\frac{2e^2}{\pi^2}\left[\frac{z_0}{d_0}\right]^2 v_c\frac{(DJ)^2}{p_0^6}\frac{q(T)^2F(\Theta/T)E_F^3}{dv_s\Gamma}\ . \tag{2.13}$$

Inserting the following set of parameters (D from Ref. 23, v_s from Refs. 18 and 22),

$$D=4\ \text{eV},\quad v_s=2.5\times10^5\ \text{cm/sec},\quad z_0=d_0=10\ \text{Å}\ ,$$
$$J=0.005\ \text{eV},\quad E_F=0.8\ \text{eV}\ , \tag{2.14}$$
$$\Gamma=1.2\times10^{-15}\ \text{ergs},\quad T=100\ \text{K},\quad d=2.5\ \text{g/cm}^3\ ,$$

into Eq. (2.13), we obtain

$$\rho_c=28(1/F)\ \Omega\,\text{cm}\ . \tag{2.15}$$

Since $F(\Theta/T)\lesssim1$, then $(\sigma_c)_{\rm LO}\gg(\sigma_c)_{\rm LA}$ if the charge-transfer factor f is not so small.

III. IMPURITY-ASSISTED HOPPING, CONDUCTION-PATH MECHANISM, AND SCATTERING BY STACKING FAULTS

In the previous paper,[10] $(\sigma_c)_I$ was obtained as

$$(\sigma_c)_I\simeq\frac{\pi z_0^2}{4\hbar I_c}\left[\frac{N_I}{N}\right]\left[\frac{JZe}{p_0}\right]^2\frac{\sum_s(E_F-\Delta_s)^3}{\left[\sum_s(E_F-\Delta_s)\right]^2}\left[\frac{1}{\Gamma}\right]\ , \tag{3.1}$$

where N_I denotes the number of ionized impurity centers and Z is the effective nuclear charge of the centers. The simple two-dimensional band model $E_s(k)=p_0k+\Delta_s$ is employed. As mentioned in Sec. II, the factor $1/\Omega$ in Eq. (2.1) should be replaced by $(I_c/d_0)(1/\Omega)$; then Eq. (3.1) becomes

$$(\sigma_c)_I\simeq\frac{\pi z_0^2}{2\hbar d_0}\left[\frac{N_I}{N}\right]\left[\frac{JZe}{p_0}\right]^2\frac{\sum_s(E_F-\Delta_s)^3}{\left[\sum_s(E_F-\Delta_s)\right]^2}\left[\frac{1}{\Gamma}\right]\ , \tag{3.2}$$

where an extra factor of 2 is multiplied in consideration of the processes (A′) and (B′) which were disregarded in the previous calculation (see Appendix). Equation (3.2) is estimated for the stage-1 Rb-Bi GIC's. The a-axis resistivity $\rho_a(T=0)\simeq0.4\ \mu\Omega$ cm in Fig. 5 leads to

$$\Gamma=4\times10^{-16}\ \text{ergs}\ . \tag{3.3}$$

From Eq. (3.3) and

$$E_F=0.8\ \text{eV},\quad N_I/N=2\times10^{-3}\ ,$$
$$z_0=d_0=10\ \text{Å},\quad Z=2\ , \tag{3.4}$$

we have

$$(\rho_c)_I(T=0)=0.19\ \Omega\,\text{cm}\ . \tag{3.5}$$

This approach provides a correct order of magnitude of $\rho_c(T=0)$ for the stage-2 $FeCl_3$ GIC in Fig. 1 and for the upper curve of the stage-1 Rb-Bi GIC in Fig. 3.

At low temperatures where the scattering due to structural imperfections makes a dominant contribution, Γ is temperature independent. With increasing temperature the phonon scattering becomes important and Γ increases. This explains the qualitative feature of the resistivity in low-stage compounds except the appearance of the maximum in alkali-metal–bismuth ternary compounds and in fluorine GIC's (see Figs. 1, 3, and 4). At high temperature ($T\gg\Theta$) $(\sigma_c)_{\rm LO}$ provides the same temperature dependence as that of $(\sigma_c)_I$ [see Eq. (2.5)].

Although the conduction-path mechanism proposed by Shimamura[11] is a physically different process from the impurity-assisted hopping, both mechanisms give rise to the same temperature dependence. Shimamura assumed that the existence of the conduction paths (conduction channels) across layers are caused by structural imperfections. The expression derived by Shimamura is, however, not appropriate for comparing with the observed results. Then, a more convenient formula is derived in the following. The scattering potential is assumed in the form

$$V=N^{-1/2}\sum_\alpha V(z,r)\Delta(r-R_\alpha)\ , \tag{3.6}$$

where $\Delta(r-R_\alpha)$ represents a two-dimensional Kronecker delta function. Since the transition rate across the conduction paths is given by

$$\frac{N_0}{N}\left|\frac{V_0}{\hbar}\right|^2\tau_{\rm coll}\quad(\hbar/\Gamma=\tau_{\rm coll})\ , \tag{3.7}$$

where N_0 is the conduction-path number and V_0 is the matrix element for V, the conductivity $(\sigma_c)_{I'}$ becomes

$$(j_c)_{I'}=(\sigma_c)_{I'}E$$
$$=\frac{ez_0}{\Omega_c}\frac{N_0}{N}\left|\frac{V_0}{\hbar}\right|^2\tau_{\rm coll}\sum_k\left[-\frac{\partial f_0}{\partial E_k}\right]eEz_0\ , \tag{3.8}$$

where $\Omega_c=(d_0/I_c)\Omega$. By using the simple two-dimensional band model Eq. (3.8) becomes

$$(\sigma_c)_{I'}=\frac{2e^2z_0}{\pi}\left[\frac{\sum_s k_{Fs}}{p_0}\right]\left[\frac{N_0}{N}\right]\frac{|V_0|^2}{\hbar\Gamma}\ , \tag{3.9}$$

where $z_0=d_0$ is inserted. Though we have no information on the magnitude of V_0, we tentatively employ the following set of parameters:

$$V_0=0.02 \text{ eV}, \quad N_0/N=10^{-3}, \quad z_0=10 \text{ Å}, \quad \sum_s k_{Fs}=2\times10^7 \text{ cm}^{-1}, \quad \Gamma=4\times10^{-16} \text{ ergs}, \tag{3.10}$$

and then we have

$$(\rho_c)_{I'}=0.28 \ \Omega \text{ cm}, \tag{3.11}$$

which is comparable to $(\rho_c)_I$ given by Eq. (3.5).

The interlayer phonon-assisted hopping proposed by Shimamura[11] is unimportant, because an effective electron-phonon interaction constant is roughly given by

$$D_{\text{eff}} \approx D e^{-z_0/c^*}, \tag{3.12}$$

where c^* is an extension of the wave function of the π electrons along the c axis, which is expected to be $z_0/c^* \gg 1$. Accordingly, we have $D_{\text{eff}} \ll D$ and the calculated conductivity σ_c is negligibly small.

By adding the four contributions discussed in Secs. II and III, $\rho_c(\text{GIG})$ is expressed as

$$\rho_c(\text{GIG})=[(\sigma_c)_{\text{LO}}+(\sigma_c)_{\text{LA}}+(\sigma_c)_I+(\sigma_c)_{I'}]^{-1}. \tag{3.13}$$

The sequence of the magnitudes for the various contributions is as follows:

$$(\sigma_c)_I+(\sigma_c)_{I'}>(\sigma_c)_{\text{LO}}+(\sigma_c)_{\text{LA}}, \tag{3.14}$$

and

$$(\sigma_c)_{\text{LO}} \gg (\sigma_c)_{\text{LA}}, \tag{3.15}$$

where the condition of Eq. (3.15) is realized for the compounds with a large charge-transfer factor f, except at low temperature ($T \ll \Theta$). Neglecting $(\sigma_c)_{\text{LA}}$, we obtain $\rho_c(\text{GIG})$ as

$$\rho_c(\text{GIG}) \simeq \Gamma(T)(a_p N_p T^{-1}+a_I+a_{I'})^{-1}, \tag{3.16}$$

where $N_p=(e^{\Theta/T}-1)^{-1}$ and a_p, a_I, and $a_{I'}$ are temperature independent. At high temperature ($T \gg \Theta$) $\rho_c(\text{GIG})$ is proportional to $\Gamma(T)$, which shows a metallic temperature dependence.

To obtain the total resistivity ρ_c represented by Eq. (2.4), it is necessary to estimate $\rho_c(\text{GG})$. In high-stage compounds $\rho_c(\text{GG})$ is approximated by the resistivity in pristine graphite. As was pointed out by Ono,[12] the reflection of electron waves at stacking faults plays an essential role in the c-axis conduction of graphite and an effective relaxation time is given by

$$\tau_{\text{eff}}=\tau[1+(R/T)(2l/L)]^{-1}, \tag{3.17}$$

where T and R denote the transmission and reflection coefficients for an electron wave at stacking faults, τ and l are the usual relaxation time and mean free path without stacking faults, and L is a mean distance between stacking faults.[12] The stacking faults associated with the basal dislocation ribbon give the most effective electron scattering mechanism ($R \simeq 1$, $T \simeq 0$), among the various types of faults.[12,27] A typical experimental result in graphite is shown in Fig. 6.[14] The resistivity decrease above ~ 50 K cannot be accounted for by Ono's theory. Wave functions on both sides of a stacking fault are smoothly connected by introducing the Tamm states, which are localized in the vicinity of the stacking fault, in addition to the Bloch state.[12] This implies that the stacking faults are equivalent to a potential barrier with a width of one lattice spacing. Ono's calculation corresponds to the tunneling effect without any activation energy; however, at finite temperature, the phonon-assisted thermal activation process takes place. The latter process becomes important at finite temperature, if the activation energy (barrier height) ΔE is not so large. Accordingly, the conductivity is composed of two parts:

$$\sigma_c=(\sigma_c)_T+(\sigma_c)_A, \tag{3.18}$$

where $(\sigma_c)_T$ stands for the tunneling effect contribution and $(\sigma_c)_A$ denotes the thermal activation part which is assumed in the form

$$(\sigma_c)_A=A[\exp(\Delta E/k_B T)-1]^{-1}. \tag{3.19}$$

To explain Fig. 6, ΔE is estimated to be ~ 100 K. This is consistent with a theoretical prediction, since ΔE is expected to be on the order of Δ ($\simeq -0.008$ eV, Ref. 28) which denotes a difference in crystalline fields experienced by inequivalent carbon atoms in layer planes. If the same mechanism is expected to be operative in GIC's, then we have

$$\rho_c(\text{GG}) \simeq [(\sigma_c)_T+(\sigma_c)_A]^{-1}. \tag{3.20}$$

Combining Eq. (3.13) with Eq. (3.20), one obtains

$$\rho_c \simeq \frac{1}{n}[\rho_c(\text{GIG})+(n-1)\rho_c(\text{GG})]. \tag{3.21}$$

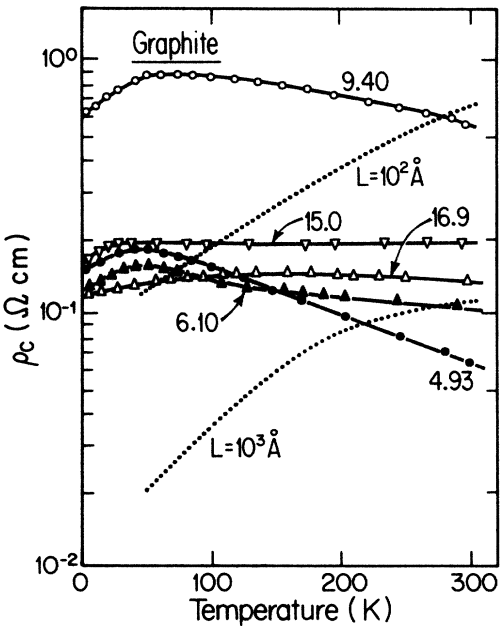

FIG. 6. Temperature dependence of the c-axis resistivity for various graphite samples, and two theoretical curves due to Ono corresponding to the stacking fault spacing $L=10^2$ and 10^3 Å, respectively. The number in each curve denotes the RRR value defined by $\rho_a(300 \text{ K})/\rho_a(4.2 \text{ K})$ (Ref. 14).

IV. COMPARISON WITH THE EXPERIMENTAL RESULTS

In low-stage compounds $\rho_c(\mathrm{GIG}) \gg \rho_c(\mathrm{GG})$, then we have

$$\rho_c \simeq \frac{1}{n}\rho_c(\mathrm{GIG}) \simeq \frac{1}{n}[(\sigma_c)_{\mathrm{LO}}+(\sigma_c)_I+(\sigma_c)_{I'}]^{-1} = \frac{1}{n}\frac{\hbar}{\tau_{\mathrm{coll}}}\{a_p[T(e^{\Theta/T}-1)]^{-1} + a_I + a_{I'}\}^{-1} . \tag{4.1}$$

Accordingly, we have

$$\rho_c \simeq \begin{cases} \frac{1}{n}\frac{\hbar}{\tau_{\mathrm{coll}}}(a_I+a_{I'})^{-1}, & T \ll \Theta \\ \frac{1}{n}\frac{\hbar}{\tau_{\mathrm{coll}}}(a_p\Theta^{-1}+a_I+a_{I'})^{-1}, & T \gg \Theta . \end{cases} \tag{4.2}$$

As mentioned in Sec. II, τ_{coll} $(=\hbar/\Gamma)$ is not identical to the relaxation time associated with the in-plane resistivity and $1/\tau_{\mathrm{coll}}$ does not include the factor $1-\cos\theta_{k,k'}$ which limits the forward scattering. Since the factor $1-\cos\theta_{k,k'}$ introduces an additional temperature dependence to ρ_a in the phonon scattering region, the temperature dependence of ρ_c is smaller than that of ρ_a. Most of GIC's satisfy this condition. Though Eq. (4.1) cannot account for the appearance of the maximum in ρ_c versus T curve for the low-stage alkali-metal–Bi ternary compounds[4–7] and for the low-stage fluorine compounds[8] (see Figs. 3 and 4), it can explain the metallic behavior of ρ_c which is a common feature in low-stage GIC's (see Fig. 1) and its order of magnitude by using a reasonable set of parameters.

In high-stage compounds the $\rho_c(\mathrm{GG})$ term is more important than the $\rho_c(\mathrm{GIG})$ and

$$\rho_c \simeq \frac{n-1}{n}\rho_c(\mathrm{GG}) = \frac{n-1}{n}[(\sigma_c)_T+(\sigma_c)_A]^{-1} , \tag{4.3}$$

which can qualitatively explain the observed temperature dependence in high-stage compounds (see Figs. 2 and 3).

V. CONCLUSIONS

The previous calculation on the c-axis conductivity in graphite intercalation compounds[10] is revised and extended in this paper. Shimamura's theory[11] on the conduction-path mechanism is reformulated. For the stage-n compounds the resistivity ρ_c is approximated by

$$\rho_c \simeq \frac{1}{n}[\rho_c(\mathrm{GIG})+(n-1)\rho_c(\mathrm{GG})] , \tag{5.1}$$

where $\rho_c(\mathrm{GIG})$ corresponds to the resistivity for the graphite-intercalant-graphite sandwich unit and $\rho_c(\mathrm{GG})$ represents the interior layer contribution to the resistivity.

(i) In low-stage compounds $\rho_c(\mathrm{GIG}) \gg \rho_c(\mathrm{GG})$ and $\rho_c(\mathrm{GIG})$ is composed of the phonon-assisted and impurity-assisted hopping processes and the conduction-path mechanism. These terms qualitatively explain the observed metallic behavior of ρ_c in low-stage compounds.

(ii) In high-stage compounds $\rho_c(\mathrm{GG})$ term is important, where it is composed of the two contributions:

$$\rho_c(\mathrm{GG}) = [(\sigma_c)_T+(\sigma_c)_A]^{-1} . \tag{5.2}$$

$(\sigma_c)_T$ is the conductivity associated with the tunneling effect at the stacking faults without any activation energy,[12] while $(\sigma_c)_A$ denotes the thermally activated conductivity. At low temperatures the $(\sigma_c)_T$ term is important and then ρ_c is temperature independent. At high temperatures ρ_c decreases with increasing temperature due to $(\sigma_c)_A$, which is proportional to $[\exp(\Delta E/k_BT)-1]^{-1}$. Therefore, Eq. (5.2) qualitatively explain the observed temperature dependence in high-stage compounds.

The presence of the maximum in the ρ_c versus T curve for the low-stage alkali-metal–Bi ternary compounds and for the low-stage fluorine compounds cannot be explained by the present theory. Further investigations are necessary experimentally and theoretically.

ACKNOWLEDGMENTS

The author would like to express his sincere thanks to Professor M. S. Dresselhaus for her careful reading of this manuscript and for valuable comments. This work was supported by the U. S. Air Force Office of Scientific Research Contract No. F49620-83-C-0011.

APPENDIX

The hopping rate across the intercalant layers W in Eq. (2.2) is expressed as follows:[10]

$$W(n,k \to n+1,p) = \frac{2\pi}{\hbar}\sum_i \left| \frac{\langle n,k \mid \mathcal{H}' \mid i\rangle\langle i \mid \mathcal{H}' \mid n+1,p\rangle}{\varepsilon(k)-\varepsilon(i)+i\Gamma} \right|^2 \times \delta(\varepsilon(k)-\varepsilon(p)+eEz_0) , \tag{A1}$$

where k, i, and p represent the electron and phonon states and Γ is a collision broadening controlled by the interactions with the phonons and impurities in the basal plane. The Hamiltonian is given by

$$\mathcal{H} = \mathcal{H}_0 + \mathcal{H}' , \tag{A2}$$

where

$$\mathcal{H}_0 = \sum_n \sum_k E(k) a_k^\dagger(n) a_k(n) + \sum_q \hbar\omega_q (b_q^\dagger b_q + \tfrac{1}{2}) , \tag{A3}$$

$$\mathcal{H}' = \mathcal{H}_{\mathrm{tr}} + \mathcal{H}_{e\text{-ph}} + \mathcal{H}_I ,$$

$$\mathcal{H}_{\mathrm{tr}} = N^{-1/2}\sum_n \sum_{k,k'} J(\mathbf{k}-\mathbf{k}')[a_{k'}^\dagger(n+1)a_k(n) + a_k^\dagger(n)a_{k'}(n+1)] , \tag{A4}$$

$$\mathcal{H}_{e\text{-ph}} = \mathcal{H}_{e\text{-LA}} + \mathcal{H}_{e\text{-LO}} , \tag{A5}$$

$$\mathcal{H}_I = \frac{4\pi e^2 Z}{\Omega\kappa}\sum_n \sum_q \frac{e^{i\mathbf{q}\cdot(\mathbf{r}-\mathbf{R}_n)}}{q^2+\lambda^2} . \tag{A6}$$

$\mathcal{H}_0$ is the unperturbed Hamiltonian, n an index denoting a graphite layer, and $\mathcal{H}_{\rm tr}$ is the transfer Hamiltonian across the intercalated layers. The indices specifying the band and phonon branches are omitted in Eqs. (A3) and (A4). N is the number of unit cells, where a unit cell is defined as the volume including two carbon atoms which sandwich an intercalated layer. (In the previous paper[10] N was incorrectly taken as the carrier density.) $\mathcal{H}_{e\text{-LA}}$ represents the electron–LA-phonon interaction associated with the out-of-plane vibration,[10] and $\mathcal{H}_{e\text{-LO}}$ is the electron–LO-phonon interaction. $\mathcal{H}_I$ denotes the ionized impurity potential, where κ is the dielectric constant, λ the screening constant, Z the effective nuclear charge, and Ω is the sample volume.

Equation (A1) includes the following four processes:

$$(A)\quad |n,k\rangle\rightarrow|n,p'\rangle,\quad |n,p'\rangle\rightarrow|n+1,p\rangle\ ;$$

$$(A')\quad |n,p'\rangle\rightarrow|n+1,p\rangle,\quad |n,k\rangle\rightarrow|n,p'\rangle\ ;$$

$$(B)\quad |n,k\rangle\rightarrow|n+1,p'\rangle,\quad |n+1,p'\rangle\rightarrow|n+1,p\rangle\ ;$$

$$(B')\quad |n+1,p'\rangle\rightarrow|n+1,p\rangle,\quad |n,k\rangle\rightarrow|n+1,p'\rangle\ .$$

In the previous theory[10] processes (A) and (B) were taken into account, while (A') and (B') were disregarded. Each process makes the same contribution to σ_c. $\mathcal{H}_{e\text{-LA}}$ and $\mathcal{H}_{e\text{-LO}}$ are given by

$$\mathcal{H}_{e\text{-LA}}=iD\sum_q\left[\frac{\hbar}{2d\Omega\omega_q}\right]^{1/2}(\hat{\mathbf{e}}\cdot\mathbf{q})\times(b_q^\dagger e^{i(\mathbf{q}\cdot\mathbf{r}-\omega t)}-b_q e^{-i(\mathbf{q}\cdot\mathbf{r}-\omega t)})\ , \tag{A7}$$

where the polarization is taken for $\mathbf{e}$ parallel to the c axis and $\omega_q\simeq v_s|q_z|$. The interaction between the carriers and the LO phonons with wave vector q is given by

$$\mathcal{H}_{e\text{-LO}}=\frac{8\pi iee^*}{v_c}\sum_q\left[\frac{\hbar}{2d^*\Omega\omega}\right]^{1/2}\frac{(\hat{\mathbf{e}}\cdot\mathbf{q})}{q^2}\times(b_q^\dagger e^{i(\mathbf{q}\cdot\mathbf{r}-\omega t)}-b_q e^{-i(\mathbf{q}\cdot\mathbf{r}-\omega t)})\ , \tag{A8}$$

where $\hat{\mathbf{e}}$ is parallel to the c acis. The dispersion $\omega(q)$ is neglected and we assume that $\omega\simeq\omega_{\rm LO}=$const. Equation (A8) is valid in the long-wavelength approximation. For simplicity the stage-1 compounds are treated in the following discussion. Here, v_c is the unit cell which is defined as the volume including two carbon atoms sandwiched by intercalant layers:

$$v_c=\frac{3^{1/2}}{2}a^2I_c,\quad a=2.46\ \text{Å}\ , \tag{A9}$$

where I_c represents the c-axis repeat distance. d^* stands for the effective density associated with the LO vibration and is given by

$$d^*\Omega=M^*N\ , \tag{A10}$$

where N is the total number of unit cells and M^* is the reduced mass defined by

$$\frac{1}{M^*}=\frac{1}{2M(c)}+\frac{n}{2M(I)}\simeq\frac{1}{2M(c)}\ , \tag{A11}$$

where $M(c)$ is the mass of a carbon atom and $M(I)$ the mass of an intercalant atom or molecule. In Eq. (A11) the chemical formula for the GIC is assumed to be C_nI. e^* in Eq. (A8) is the charge located on two carbon atoms which are included in the unit-cell volume v_c. Accordingly, e^* takes the form

$$\frac{e^*}{e}=\frac{2f}{n}\ , \tag{A12}$$

where f is the charge-transfer factor per intercalant.

[1] J. P. Issi, B. Poulert, J. Heremans, and M. S. Dresselhaus, Solid State Commun. **49**, 449 (1982).

[2] D. T. Morelli and C. Uher, Phys. Rev. B **27**, 2477 (1983).

[3] J. E. Fischer, C. D. Fuerst, and H. J. Kim, in *Intercalated Graphite*, Vol. 20 of *Materials Research Society, Symposia Proceedings, Boston, 1982*, edited by M. S. Dresselhaus, G. Dresselhaus, J. E. Fischer, and M. J. Moran (North-Holland, New York, 1983), p. 169.

[4] J. F. Mareche, E. McRae, A. Bendriss-Rehehaye, and P. Lagrange, J. Phys. Chem. Solids **47**, 477 (1986).

[5] E. McRae, J. F. Mareche, A. Bendriss-Rehehaye, P. Lagrange, and M. Lelaurain, Ann. Phys. (Paris), Colloq., Suppl. 2 **11**, 13 (1986).

[6] N. E. Nadi, E. McRae, J. F. Mareche, M. Lelaurain, and A. Herold, Carbon **24**, 695 (1986).

[7] E. McRae, J. Mareche, and A. Herold, in *Extended Abstract of the Symposium on Graphite Intercalation Compounds at the Materials Research Society Meeting, Boston, 1986*, edited by M. S. Dresselhaus, G. Dresselhaus, and S. Solin (MRS, Pittsburgh, 1986), p. 152.

[8] H. Touhara (unpublished).

[9] Y. Ohta, K. Kawamura, and T. Tsuzuku, J. Phys. Soc. Jpn. **55**, 2338 (1986).

[10] K. Sugihara, Phys. Rev. B **29**, 5872 (1984).

[11] S. Shimamura, Synth. Met. **12**, 365 (1985).

[12] S. Ono, J. Phys. Soc. Jpn. **40**, 498 (1976).

[13] G. J. Morgan and C. Uher, Philos. Mag. B **44**, 427 (1981).

[14] T. Tsuzuku, Carbon **21**, 415 (1983).

[15] L. Pietronero, S. Strassler, and H. R. Zeller, Phys. Rev. Lett. **11**, 763 (1978).

[16] S. Shimamura and A. Morita, J. Phys. Soc. Jpn. **51**, 5021 (1982).

[17] T. Ohno and H. Kamimura, J. Phys. Soc. Jpn. **52**, 223 (1983).

[18] P. C. Eklund and G. Giergiel, in *Physics of Intercalation Compounds*, edited by L. Pietronero and E. Tosatti (Springer-Verlag, Berlin, 1981), p. 168.

[19] A. Magerl and H. Zabel, in *Physics of Intercalation Compounds*, Ref. 18, p. 180.

[20] P. C. Eklund, J. L. Zeretsky, and W. A. Kamitakahara (unpublished).

[21] W. A. Kamitakahara, H. Zabel, and R. M. Nicklow, in *Intercalated Graphite*, Vol. 20 of *MRS Symposia Proceedings*, edit-

ed by M. S. Dresselhaus, G. Dresselhaus, J. E. Fischer, and M. J. Morgan (North-Holland, New York, 1983), p. 323.

[22]D. M. Hwang and B. F. O'Donnell, in *Physics of Intercalation Compounds,* edited by L. Pietronero and E. Tossati (Springer-Verlag, Berlin, 1981), p. 193.

[23]S. Ono and K. Sugihara, J. Phys. Soc. Jpn. **21**, 861 (1966).

[24]K. Sugihara, in *Extended Abstracts of the Symposium on Graphite Intercalation Compounds at Materials Research Society Meeting, Boston, 1984,* edited by P. C. Eklund, M. S. Dresselhaus, and G. Dresselhaus (MRS, Pittsburgh, 1984), p. 60.

[25]Y. Ohta, Ph.D. thesis, Nihon University, 1987 (in Japanese).

[26]H. Kamimura, K. Nakao, T. Ohno, and T. Inoshita, Physica B + C **99B**, 401 (1980).

[27]S. Amelinckx, P. Delavigntee, and M. Heershap, in *Chemistry and Physics of Carbon,* edited by P. L. Walker, Jr. (Dekker, New York, 1965), Vol. 1, p. 1.

[28]M. S. Dresselhaus and G. Dresselhaus, Adv. Phys. **30**, 139 (1981).